Journal of Applied Electrochemistry (2005) 35:9–15
DOI 10.1007/s10800-004-1760-7

Effect of WC on electrodeposition and corrosion behaviour of chromium coatings

S. SURVILIENE[1]*, V. JASULAITIENE[1], A. LISOWSKA-OLEKSIAK[2] and V.A. SAFONOV[3]
[1]*Institute of Chemistry, A. Gostauto 9, 01108 Vilnius, Lithuania*
[2]*Technical University of Gdansk, G.Narutowicza 11/12, 80952 Gdansk, Poland*
[3]*Moscow State University, Vorob'evy gory, GSP-3, 119899 Moscow, Russia*
*(*author for correspondence, e-mail: Sveta@ktl.mii.lt)*

Received 11 March 2004; accepted in revised form 14 July 2004

Key words: chromium coating, corrosion, cyclic polarization, impedance spectroscopy, steel, WC particles

Abstract

To study the effect of WC particles on corrosion behaviour of chromium coating steel samples were plated in Cr(VI) baths with various concentrations of WC. XPS, EPM and XRD were used to study the chemical composition, morphology and texture of the coatings. The corrosion behaviour was studied at different exposure times in solution containing $0.01\,mol\,L^{-1}$ H_2SO_4 + $0.5\,mol\,L^{-1}$ Na_2SO_4 using cyclic voltammetry and impedance spectroscopy. Cyclic polarization measurements suggest that WC particles slow down the processes of passive film dissolution and penetration of aggressive ions to the substrate. Electrochemical impedance spectroscopy (EIS) was used to reveal the details of the corrosion process at the solution/electrode interface. The simulation of EIS data with a proposed equivalent circuit model made it possible to obtain quantitative valuation of the Y_0 (Q_c), Y_0 (Q_s) and R_{pore} parameters, reflecting corrosion behaviour of samples at the solution/electrode interface. Samples plated in a Cr(VI) bath with WC provided better resistance to corrosion than those plated in a bath without WC. Analysis of the data obtained suggests that WC particles enhance corrosion resistance due to the microstructural features of the coatings.

1. Introduction

The use of various dispersion particles as an additive to Cr(VI) baths is one of the most technologically reliable and cost-effective techniques to improve protective properties of coatings. Co-deposition of particles may significantly enhance the existing characteristics and even add entirely new properties [1]. The low content of the particles incorporated in Cr coating from hexavalent chromium electrolyte may be associated with such factors as intensive evolution of hydrogen and the presence of a cathodic film. In spite of this, the addition of the dispersed particles to the Cr(VI) bath may cause a transformation in the matrix of the coating. The particles affecting Cr matrix morphology may promote deposition of coatings with excellent corrosion resistance [2].

Cyclic voltammetry and EIS are widely used to investigate protective properties of the coatings [3–6]. Impedance measurements are based on the determination of impedance spectra in a wide range of frequencies for various coating exposure times to the aggressive solution. Although modelling and interpretation of EIS data is difficult and lengthy, it is essential for the EIS study on electrochemical corrosion. In particular, the variation of some parameters with immersion time correlates with the corrosion behaviour of plated system [4–5].

The aim of this work was to study the effect of WC particles on both the chromium electrodeposition and corrosion properties of the coatings.

2. Experimental details

Chromium coatings were plated on steel containing 99.4% iron (Steel-3) in solution containing $120\,g\,L^{-1}$ of chromic anhydride (CrO_3), $2.5\,g\,L^{-1}$ of Limeda Ch-3 additive, which is a mixture of fluoride-containing complexes and sulphate compounds [7], and additionally WC particles (with dimensions of about 1 μm). The solution was agitated before electrolysis for over 4 h. The steel cathode was mechanically polished, degreased with magnesium oxide, rinsed thoroughly, activated in dilute (1:1) hydrochloric acid and then rinsed with deionised water. A bath with a volume of 1:1 with two vertical anodes and a steel cathode between them was maintained at constant temperature and agitated with a $150\,L\,h^{-1}$ flow of compressed air. Anodes were made from Pb alloy containing 7% Sn. The samples were plated during 20 min at a current density (i_c) of 40 $A\,dm^{-2}$ and a temperature of 50 °C. The electrodepos-

ition rate (V_{Cr}) was determined by the gravimetric method.

Thermal effects on microhardness of the coatings were investigated after annealing the samples at 200 and 600 °C for 6 h. Vicker's microhardness (HV) was measured using a 50 g load on 20 μm thick coatings and the average value was calculated from over 10 measurements.

Corrosion resistance of samples plated in baths with and without WC particles was tested in a neutral salt spray chamber. The temperature in the test chamber was maintained at 35 ± 2 °C. Corrosion resistance of the coatings (10 μm) was evaluated as a percentage of the area of defects in the coatings according to the ISO 4540 standard [8].

The electrochemical measurements were carried out in a three-electrode cell of 100 cm^3. A steel plate covered with chromium coating was used as a working electrode. A platinum plate and a saturated calomel electrode (SCE) were used as counter and reference electrodes, respectively. All the potentials given are referred to the SCE. All measurements were performed in solution containing 0.01 mol L^{-1} H_2SO_4 and 0.5 mol L^{-1} Na_2SO_4. Cyclic polarization measurements were conducted under potentiodynamic conditions with a potential scan rate of 10 mV s^{-1} at a temperature of 20 ± 1 °C. The polarization was usually carried out in the positive direction and then reversed to the initial potential.

The composition of both the substrate and the coating in wt % was determined by means of an X-ray electron probe microanalyzer JXA-50A. The morphology of coatings was studied by SEM.

Elemental analysis of coatings was carried out using X-ray photoelectron spectroscopy (XPS). The spectra were recorded by an ESCALAB MK-II spectrometer (VG Scientific, UK) using MgK_α anode radiation (1253 eV, a pass energy of 20 eV). The quantity of each element in at. % was calculated from the single Cr2p, C1s, O1s and W2p peaks areas. Empirical sensitivity factors of the elements were taken from [9] and the spectra recorded were compared with the standard ones [10]. Some of samples were examined by the X-ray diffraction (XRD) method.

Measurements of electrochemical impedance were carried out at the open circuit potential (E_{corr}) after immersion of a sample into solution for different time periods (from 30 s to 7 days). The Autolab combined with GPES software provided a fully computer controlled electrochemical measurement system. Frequencies were varied from 2×10^4 to 5×10^{-2} Hz. The amplitude of sinusoidal potential was 10 mV peak to peak.

The EIS data were interpreted using an equivalent circuit model, which was proposed on the basis of the model describing the electrochemical corrosion of the coated surface. The calculated parameters of equivalent circuit were used for simulation of impedance diagrams. Finally, the data obtained were fitted and analysed using the EQUIVCRT program written by Boukamp [11].

3. Results and discussion

Table 1 shows that the presence of WC in the Cr(VI) bath leads to reduction in the electrodeposition rate (V_{Cr}), as well as the hardness (HV) of the coatings. HV remained almost unchanged after annealing at 200 °C. A sharp decrease in HV observed after 6 h annealing at 600 °C may be conditioned by recrystallization of the deposits [12].

The XRD data presented in Table 2 show that the intensities of the XRD peaks recorded for the samples plated in the bath with WC were lower than those for the samples plated in the absence of WC. Table 3 shows the percentages of crystallites oriented in the various crystallographic directions calculated according to the method described in [13].

Figure 1 shows that the samples plated in the bath with WC exhibited a much higher resistance to corrosion than those plated in the bath without WC.

In order to study the influence of WC particles on pitting corrosion, the samples were plated in baths containing 10 (a) and 20 (b) g L^{-1} of WC. The sample was dipped into a sulphate solution and potential–current curves (PC) were recorded consecutively after different immersion times (Figure 2). The initial PC exhibited a small anodic current, which may be attributed to the presence of an oxide film on the surface. The second and the third consecutive PCs demonstrated an

Table 1. Concentration of WC particles (g L^{-1}) in Cr(VI) bath, electrodeposition rate of the coating (V_{Cr}) at i_c = 40 A dm^{-2}, t = 50 °C and hardness of the coatings (HV) before and after hot treating

Number of sample	WC/ g L^{-1}	V_{Cr}/ μm min^{-1}	HV	HV	
				After heating 200 °C	600 °C
1	0	0.65	980	900	770
2	2	0.58	970	1000	620
3	5	0.50	990	930	600
4	10	0.55	930	900	540
5	20	0.54	900	865	520

Table 2. XRD data: the hkl index, integral intensity (I_{int}), interplanar distance (d) and XRD peak width (W_{FWHM})

Concentration of WC / g L^{-1} in Cr(VI) bath	hkl	I_{int} / a.u.	d / Å	W_{FWHM} / deg.
Without particles	110	17.6	2.040	0.708
	200	64.8	1.440	1.01
	211	63.2	1.176	1.446
10	110	3.1	2.042	0.577
	200	47.0	1.453	1.02
	211	24.2	1.177	1.484
20	110	0	0	0
	200	17.7	1.439	0.998
	211	5.2	1.171	1.01

Table 3. XRD data: the percentage of Cr crystallites orientated in various directions calculated for the coatings obtained in baths without (I) and with 20 g L^{-1} of WC (II)

<hkl>	I	II
110	2.8	0.0
100	63.2	86.1
211	34.0	13.9

increase in the current density. It is believed that this is a result of modification and dissolution of the protective oxide film and emergence of damages (microcracks) in the coatings, as well. Qualitatively similar PCs were obtained in argon atmosphere. The polarization behaviour of pure Cr coating in the solution studied was discussed elsewhere [14, 15]. The passive film formed on the Cr surface upon anodic oxidation in H_2SO_4 solution was identified in [16–18]. According to [17] the passive film is a thin hydrated chromic oxide (5–25 Å) that may be considered as a dielectric with a dielectric constant of 25. The decrease in current density in the potential region −0.3 to −0.2 V suggests the formation of Cr(II) oxide or hydroxide. However, XPS data suggest that the passive film on the surface of coating consists of Cr(III)-oxide and Cr(III)-oxyhydroxide. Seemingly, the oxidation of Cr(II) to Cr(III) occurs in the passive region with increasing potential: $Cr(OH)_2$(film) → CrOOH(film) + H^+ + e^-. Taking into account the data cited in [19], it may be suggested that during the negative potential sweep the reverse reaction Cr(III) → -Cr(II) occurs in the oxide film at the potential below +0.2 V. Analysis of the PCs obtained leads to the conclusion that the higher WC concentration in the Cr(VI) bath is the lower current density is observed in the region of active dissolution.

Figure 3 shows the XPS spectra for $Cr2p_{3/2}$ recorded on the outer layers of Cr deposited in baths without WC (curve 1) and with WC (curves 2–4). Two $Cr2p_{3/2}$ peaks that can be attributed to Cr^0 metallic and to Cr_2O_3, CrOOH and $Cr(OH)_3$ [16, 17] emerged in the XPS

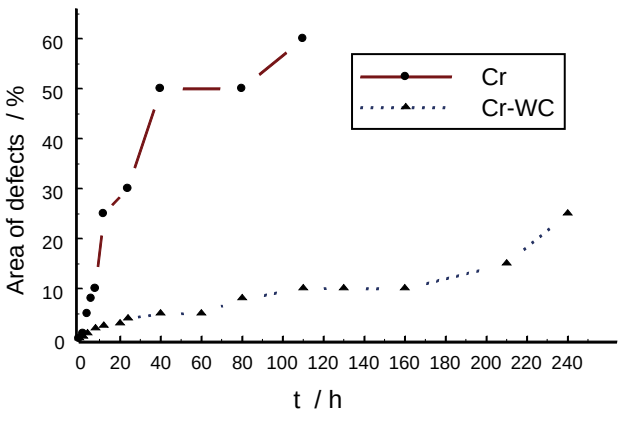

Fig. 1. Time dependences of the area of defects (%) in the coatings (10 μm) obtained in Cr(VI) baths without and with 20 g L^{-1} of WC tested in a neutral salt spray chamber.

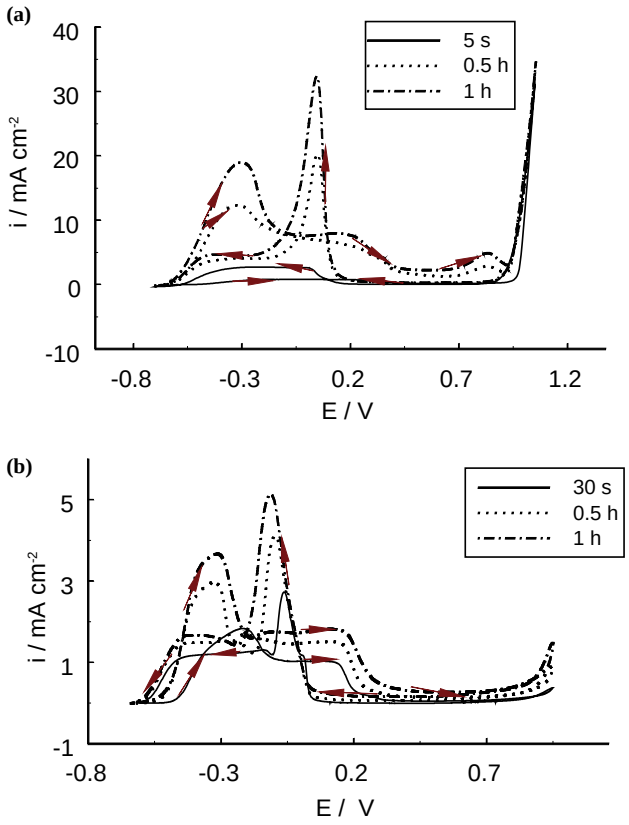

Fig. 2. Cyclic polarization curves recorded consecutively after immersion of sample in solution containing 0.01 M H_2SO_4 + 0.5 M Na_2SO_4. The samples were plated in Cr(VI) baths containing 10(a) and 20 (b) g L^{-1} of WC. The coating thickness was 10 μm.

spectra. It is seen that the peak positions for both Cr^0 and Cr(III) practically coincide in all samples. The peaks corresponding to metallic chromium and to Cr_2O_3 [10] emerged in the spectra recorded in depth (i.e., after Ar^+ ion bombardment). The $W4f_{7/2}$ signals at 35.6 ± 0.1 eV and at 33.5 ± 0.1 eV were somewhat shifted when

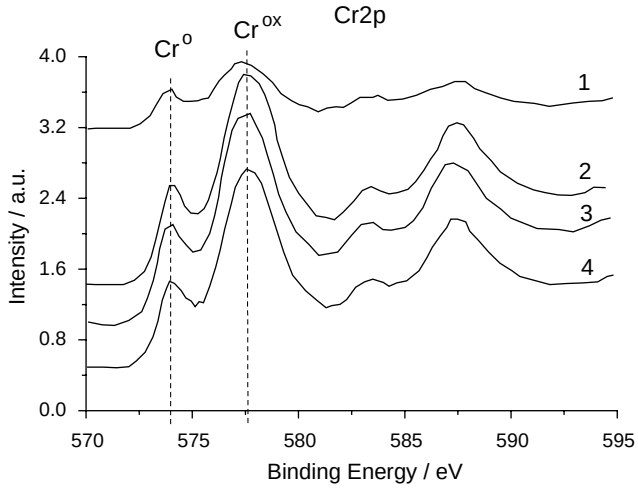

Fig. 3. XPS spectra for $Cr2p_{3/2}$ recorded on the surface of coatings obtained in Cr(VI) bath without (1) and with 10 (2), 20 (3), 50 (4) g L^{-1} of WC particles.

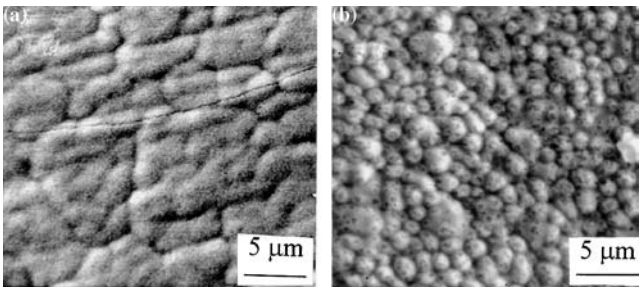

Fig. 4. Micrographs of the coatings deposited in Cr(VI) bath without (a) and with 10 g L^{-1} of WC particles (b).

compared with the peak typical of WC spectra (31.7 eV).

The quantity of WC particles in wt % (G_{dp}) was determined by EPM in the coatings deposited in the bath containing 20 g L^{-1} WC. The data obtained show very small occlusion of the particles in the deposit: about 0.15 and 0.20 wt % at thickness 10 and 20 μm, respectively. This suggests that DPs may be forced upward from the surface of the growing deposit.

The SEM data in Figure 4 show that the coating obtained in the Cr(VI) bath without WC has a fine-grained structure with microcracks whereas that one obtained in the bath with 10 g L^{-1} WC may be characterized as an spherolite with ball-like crystals structure without microcracks.

In order to study corrosion behaviour of the coating, impedance spectra were recorded at E_{corr} for various immersion times. The impedance diagrams in Figure 5 were recorded either shortly after chromium plating ((a) and (b) and (e) and (f)) or after exposure of the sample to air for one year ((c) and (d)). The data in Figure 5(c) suggest that the passive film, formed on the surface during one year of exposure to air, was destroyed in a very short time after immersion. The Niquist diagrams show greater semicircle diameters for the sample plated in the bath with 20 gL^{-1} WC ((Figure 5(a) and (b)). This suggests that WC particles enhance corrosion resistance. Increased semicircle diameter after six ((in Figure 5(b)) and after three ((in Figure 5(f)) days of exposure suggests that the products of substrate corrosion filling the defects in the coating impede penetration of the aggressive solution to the substrate. As the electrical resistance of rust is greater than that of the solution, a slight increase in impedance was induced. The plots zoomed at 15–30 ohm of impedance range (Figure 6) show that a high-frequency semi-circle can be observed in diagrams recorded after six (b) and three (f) days of exposure for the samples plated in baths containing 20 and 10 g L^{-1} of WC, respectively. The reason for this phenomenon may be the rust plugging pinholes, which was visually observed on the both surfaces.

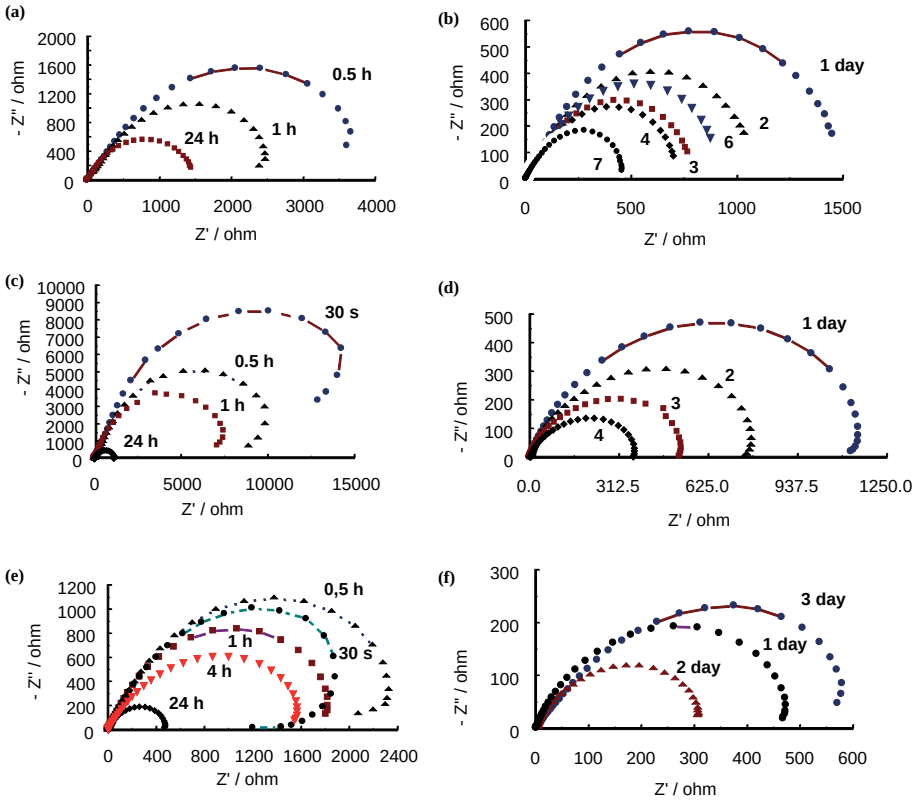

Fig. 5. Complex plan impedance diagrams of chromium coatings recorded at E_{corr} after different exposure periods to 0.01 M H_2SO_4 + 0.5 M Na_2SO_4 solution. The coatings were deposited in Cr(VI) baths containing 20 ((a), (b), (c) and (d)) and 10 ((e) and (f)) g L^{-1} of WC particles. The coating thickness was 10 μm. The data ((c) and (d)) obtained for the samples exposed to air during 1 year and than immersed into the studied solution.

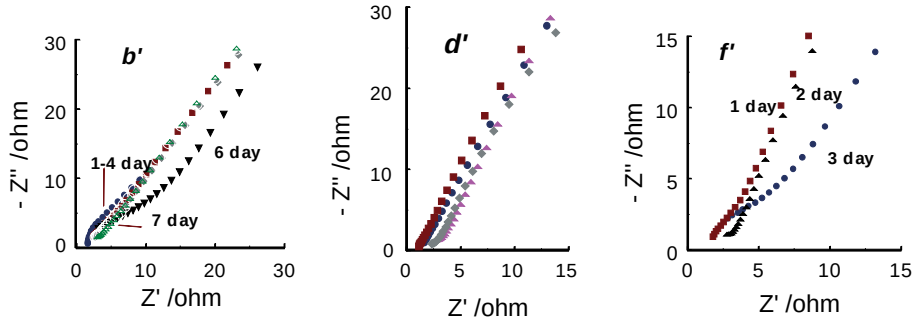

Fig. 6. Nyquist plots of EIS data zoomed at the high frequency region from Figure 5 (b), (d) and (f).

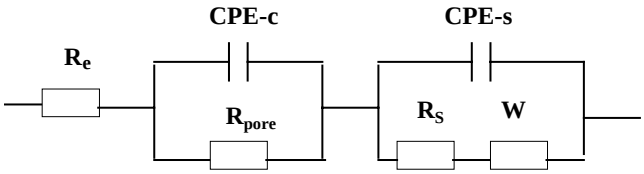

Fig. 7. Equivalent circuit used for simulation of the experimental data.

Figure 7 shows the equivalent circuit model proposed for EIS data simulation. A constant phase element (CPE) is marked as Q in circuit description code (CDC) and it is defined by twhe admittance Y and the power index number n: $Y = Y_0 (j\omega)^n$. Y_0 (Q_c) and Y_0 (Q_s) reflect the behaviour of electrolyte/coating and electrolyte/steel (via defects) interfaces. Y_0 (Q_c) and Y_0 (Q_s) become C_c and C_s for n=1, respectively. The term n shows how far the interface is from an ideal capacitor. Warburg (W) is usually used to describe diffusion. The impedance data were fitted using various equivalent circuit models that are usually used to describe corrosion processes. The equivalent circuit given in Figure 7 appears to be the best fitting of our experimental data. Fitting errors according to $R_1(Q_1R_2)(Q_2[R_3W])$ circuit were less than 10% for both real and imaginary parts of impedance. It is not improbable that a number of the smallest pinholes emerged shortly after immersion.

Tables 4 and 5 show that $n > 0.5$ and initially it is close to 1 suggesting a capacitive response from the electrolyte/coating interface. The n-Q_c value decreased with time indicated that the capacitive interface was weakened because the coating became more conductive due to the increased number of opening pinholes. This may reflect a decrease in R_{pore} with immersion time. The increase in R_{pore} may be considered as the consequence of pinhole plugging by rust.

The fitting curves are presented in Figure 8. The impedance value and the phase angle (Φ) on the Bode

Table 4. EIS data simulation for the sample plated in Cr(VI) bath with 20 g L^{-1} WC

Exposure time	E_{corr} /mV(SCE)	R_e/Ω cm^2	$Y_0(Q_c)\times10^6$ /Ω^{-1} cm^{-2} s^n	n-Q_c	R_{pore}/Ω cm^2	$Y_0(Q_s)\times10^6$ /Ω^{-1} cm^{-2} s^n	n-Q_s	R_s Ω cm^2	$Y_0(W)\times10^6$ /Ω^{-1} cm^{-2} s^{05}	i_{corr} /μA cm^{-2}
0.5 h	− 588	1.20	30.80	0.98	3055	0.596	0.84	900	125	4.2
1 h	− 583	1.20	76.50	0.99	2050	1.255	0.76	550	170	6.8
1 day	− 618	1.20	66.00	0.88	1300	1.800	0.60	220	299	10.1
2 day	− 615	1.10	51.50	0.84	1015	1.900	0.96	96.8	990	15.0
3 day	− 645	1.20	73.17	0.85	661	0.086	0.99	174	1457	21.2
4 day	− 653	1.25	97.00	0.86	600	0.090	0.99	165	1650	24.2
6 day	− 654	1.10	22.04	0.74	1039	0.036	0.99	18.3	625	17.8
7 day	− 639	1.7	78.26	0.82	403	0.008	0.99	93.9	2270	34.0

Table 5. EIS data simulation for the sample plated in Cr(VI) bath with 10 g L^{-1} WC

Exposure time	E_{corr} /mV(SCE)	R_e/Ω cm^2	$Y_0(Q_c)\times10^6$ /Ω^{-1} cm^{-2} s^n	n-Q_c	R_{pore}/Ω cm^2	$Y_0(Q_s)\times10^6$ /Ω^{-1} cm^{-2} s^n	n-Q_s	R_s Ω cm^2	$Y_0(W)\times10^6$ /Ω^{-1} cm^{-2} s^{05}	i_{corr} /μA cm^{-2}
0.5 h	− 644	1.12	61.08	0.99	1892	1.936	0.62	498.0	29	7.1
1 h	− 646	1.17	56.88	0.97	1483	2.190	0.61	440.0	32	9.4
1 day	− 655	1.40	21.35	0.81	498	7.540	0.80	26.8	1586	34.0
2 day	− 668	1.60	20.01	0.76	329	3.976	0.90	12.8	1200	54.8
3 day	− 672	1.00	10.18	0.69	692	1.151	0.99	5.9	848	28.3

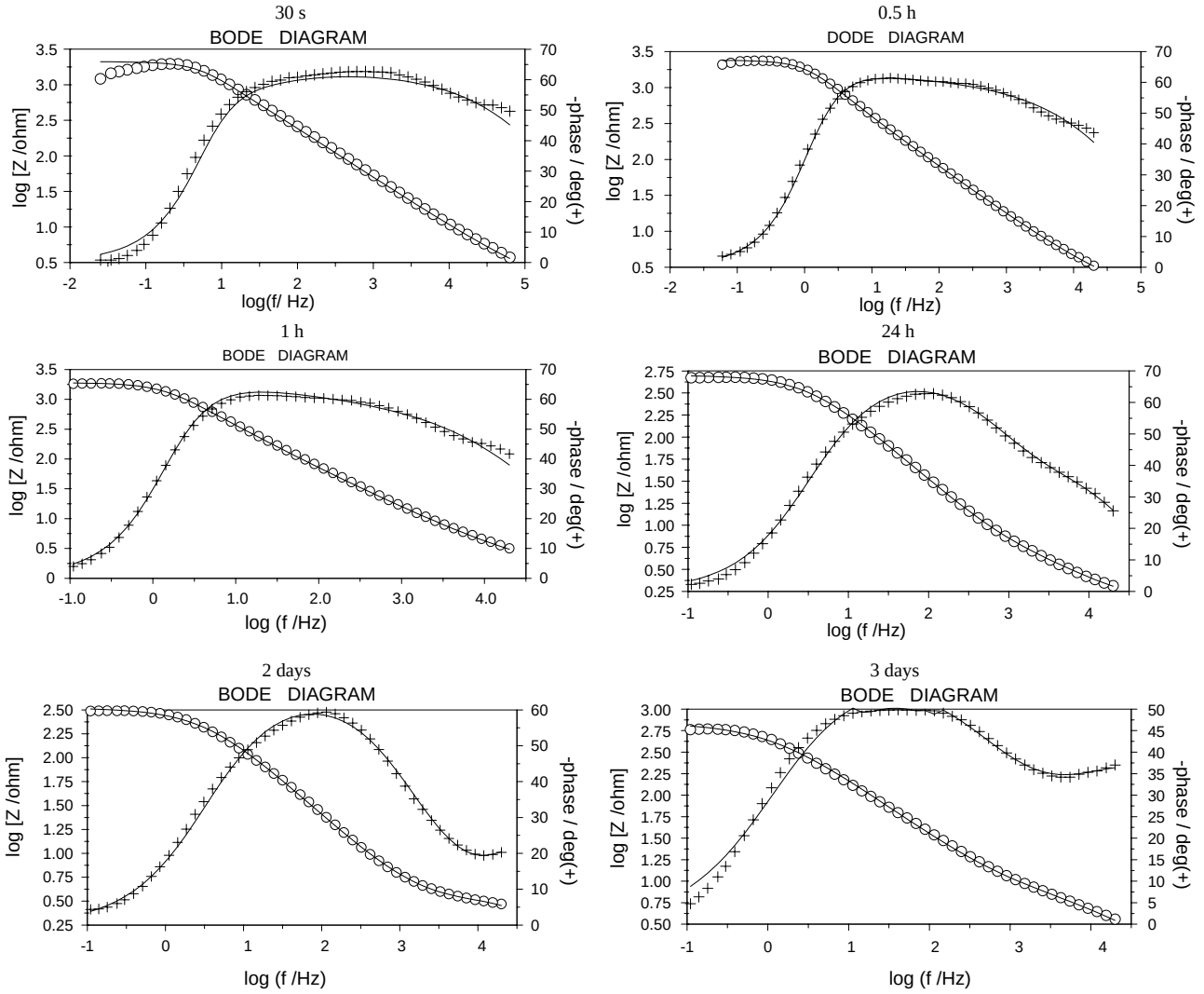

Fig. 8. Bode diagrams obtained for Nyquist plots of EIS data in Figure 5 (e) and (f). Continuous lines represent fitting of the experimental data through the equivalent circuit shown in Figure 7.

plots in the lower frequency region correspond to behaviour at the substrate/electrolyte interface [20]. In the higher frequency region Φ corresponds to behaviour of the coating [3]. The change in such parameter as the minimum phase angle (Φ_{min}) was used for the analysis of polymer-coated steel and corrosion at the metal/coating interface [21]. Bode diagrams in Figure 7 show that the impedance value at the lowest frequency decreased. No significant signs of corrosion were observed after that time of exposure. After three days corrosion products were observed on the coating surface and the impedance value increased. The Φ in the highest frequency region dropped to Φ_{min} after two days but increased after three days of exposure. This suggests that the change in Φ at highest frequencies represents qualitatively the processes occurring in the chromium coating.

According to the simplified approach, under open-circuit conditions the steady-state (corrosion) current and the polarization resistance R_p across the interface are related by the equation [22, 23]:

$$i_{corr} = \left(\frac{b_+ b_-}{2.303(b_+ + b_-)}\right)\left(\frac{1}{R_p}\right). \quad (1)$$

In the frame of the simplest model, the polarization resistance R_p is expressed as

$$R_p = |Z(j\omega)|_{\omega\to 0} - |Z(j\omega)|_{\omega\to\infty}. \quad (2)$$

Using Tafel constants $b_+ = 0.06$ V and $b_- = 0.12$ V the i_{corr} values were estimated. The data in Tables 4 and 5 show that the higher the WC concentration in the Cr(VI) bath the lower the i_{corr} in the coating obtained.

4. Conclusions

Analysis of the coatings deposited in Cr(VI) baths containing 10 and 20 g L^{-1} of WC particles has shown that the particles were incorporated in a relatively low weight percentage into Cr coatings. However, they had a

significant influence on the morphology of the Cr coating.

Cyclic polarization measurements indicated that increase in WC concentration led to a decrease in current density in the region of active dissolution. The corrosion behaviour of the samples was studied through the modelling of EIS spectra at different times of exposure to the sulphate solution. The simulation of EIS data with an proposed equivalent circuit model made it possible to obtain quantitative evaluation of the parameters $Y_0(Q_c)$, $Y_0(Q_s)$ and R_{pore}, reflecting the corrosion behaviour of the samples at the solution/electrode interface. The corrosion initiated via pinholes propagated more slowly and pinhole plugging by corrosion products occurred much later in the samples plated in the bath with a higher WC concentration. Bode plots suggest that the change in phase angle with frequency applied represents qualitatively the processes occurring in the coating and at the steel/solution interface. Analysis of the data obtained suggests that WC particles enhance corrosion resistance due to the microstructural features of the coatings.

Acknowledgement

The authors thank Dr. R. Juskienas for performing the XRD studies.

References

1. R.S. Saifullin, 'Physical Chemistry of Inorganic Polymer and Composite Materials', (Horwood Chichester, UK, 1991).
2. S. Surviliene, S. Bellozor, M. Kurtinaitiene and V.A. Safonov, *Surf. Coat. Technol.* **176** (2004) 193.
3. F. Mansfeld, *J. Appl. Electrochem.* **25** (1995) 187.
4. C. Liu, Q. Bi and A. Matthews, *Corros. Sci.* 43 (2001) 1953.
5. C. Liu, Q. Bi, A. Leyland and A. Matthews, *Corros. Sci.* **45** (2003) 1243.
6. J.R. Scully and S.T. Hensley, *Corrosion* **50** (1994) 705.
7. M.A. Mickus, S.P. Surviliene, S.Y Juknevichius and B.A. Shalkus, A.S. USSR No. 1425257. *Bul. Izobretinii*, 35, 1988 (in Russian).
8. International Standard ISO 4540. Metallic coatings - Coatings cathodic to the substrate. Rating of electroplated test specimens subjected to corrosion tests. 1980
9. D. Briggs and M.P. Seach (Eds.), Practical Surface Analysis by Auger and X-ray Photoelectron Spectroscopy, Wiley, Chichester, UK, 1983.
10. C.D. Wagner, W.M. Riggs, L.E. Davis, J.F. Moulder and G.E. Muilenberg. Handbook of X-ray Photoelectron Spectroscopy (Perkin-Elmer, Minneapolis, MN, 1978), p. 190.
11. B.A Boukamp, *J. Electrochem. Soc.* **142** (1995) 1885.
12. R.Y. Tsai and Sh.-T. Wu, *J.Electrochem. Soc.* **136**(5) (1989) 1341.
13. L.Ph. Berube and G. Esperance, *J.Electrochem. Soc.* **136** (1989) 2314.
14. A.A. Edigaryan, V.A. Safonov, E.N. Lubnin, L.N. Vykhodtseva, G.E. Chusova and Yu.M. Polukarov, *Electrochim. Acta*, **47** (2002) 2775.
15. S. Surviliene, S. Bellozor and V.A. Safonov, *Bull. Electrochem.* **18** (2002) 391.
16. V. Maurice, W.P. Yang and P. Marcus, *J. Electrochem. Soc.* **141** (1994) 3016.
17. T.P. Moffat and R.M. Latanision, *J. Electrochem. Soc.* **139** (1992) 1869.
18. M. Bojinov, G. Fabricius, T. Laitinen and T. Saario, *J. Electrochem. Soc.* **145** (1998) 2043.
19. M. Bojinov, G. Fabricius, T. Laitinen, T. Saario and G. Sundholm, *Electrochim. Acta* **44** (1998) 247.
20. L. van Leaven, M.N. Alias and R. Brown, *Surf. Coat. Technol.* **53** (1992) 25–34.
21. C.H. Tsai and F. Mansfeld, *Corros.* **49**(9) (1993) 726.
22. C. Wagner and W. Traud, *Z. Elektrochem.* 44 (1938) 391.
23. M. Stern and A.L. Geary, *J. Electrochem. Soc.* 104 (1957) 56.